DOI: 10.1002/ejic.201100451

$\{Os_5Lu_{20}\}I_{24}$, the First Extended Cluster Complex of Lutetium with Eight-Coordinate Endohedral Osmium Atoms in Two Different Environments

Matthias Brühmann,[a] Anja-Verena Mudring,[b] Martin Valldor,[c] and Gerd Meyer*[a]

Dedicated to Professor John D. Corbett on the occasion of his 85th birthday

Keywords: Cluster compounds / Synthetic methods / Rare earths / Lutetium / Osmium / Electronic structure / Magnetic properties / Endohedral atoms

$\{Os_5Lu_{20}\}I_{24}$ was obtained from a conproportionation reaction of lutetium and lutetium triiodide in the presence of osmium in an arc-welded tantalum container at 850–1200 °C. The crystal structure has been determined by single-crystal X-ray diffraction analysis. Square antiprisms and cubes of lutetium atoms in a 4:1 ratio share common square faces in a chain; they encapsulate osmium atoms and are surrounded by iodide ions. Os–Os distances within the cluster chains (299, 303, and 325 pm) imply only little if no bonding between neighbouring osmium atoms. The cluster complex chains are packed in the fashion of a hexagonal closest packing of rods. There are only van der Waals interactions between these chains as the shortest inter-chain Lu–I distances of 468 pm attest. Electronic structure calculations show mainly Os–Lu and Lu–I bonding, with lesser Lu–Lu and negligible Os–Os contributions. Remarkable is the considerable population of Lu-5d states close to the Fermi level. Susceptibility measurements show complex magnetic behavior with ferromagnetic coupling in the $\{Os_5Lu_{20}\}$ chains and antiferromagnetic coupling between the chains, which results in geometric frustration. As a consequence, the spin system has a cluster-glass-like ground state.

Introduction

The large number and variety of rare earth metal clusters that are now known exhibit distinct structural and bonding patterns.[1–3] For example: (1) almost all rare earth metal clusters $\{R_n\}$ need an endohedral atom Z (or an atom group, C_2^{6-} is a prominent one), usually from rather electronegative main-group elements or transition elements mainly from Groups 7–10; (2) isolated clusters are rare, whereas condensed metal clusters are ubiquitous and share electrons for bonding interactions; (3) the coordination number of the endohedral atom is, in the majority of cases, six, however coordination numbers of four (with O, N, C atoms), seven (Ru in $\{RuPr_3\}Cl_3$),[4] and eight (Re, Os, Ir, for example in $\{OsSc_4\}Cl_4$)[5] are increasingly observed; (4) rare earth elements that form clusters have high reduction potentials for the half cells $E°(M^{3+}/M^{2+})$, below about –2 V, and require the electronic configuration $[Xe]6s^24f^n5d^1$ over $[Xe]6s^24f^n5d^0$. These elements are Sc, Y, La, Ce, Pr, (Nd), Gd, Tb, (Dy), Ho, Er, and Lu, with Nd and Dy also forming salt-like diiodides; (5) bonding in cluster complexes $\{ZR_n\}X_m$ is dominated by Z–R and R–X interactions with considerably smaller (if any) homo-atomic Z–Z and R–R attraction – for a recent study see ref.[6]; (7) rare-earth cluster complexes may be understood as anti-Werner complexes with the (electronegative) endohedral atom Z actually the central atom surrounded by a first coordination sphere of (electropositive) R atoms and a second coordination sphere of (electronegative) X atoms; to date, X = halides.[3f]

Lutetium as the last lanthanide element with a closed 4f shell does form clusters but, as with its right-hand neighbour hafnium, the number of examples is small. These include $[\{CLu_6\}Cl_{18}]Cs_2Lu$ (an isolated cluster;[7] the most oxidized example with only nine electrons for intra-cluster bonding), $\{H_xLu\}Cl$, and $\{CLu_2\}Cl_2$ with main group atoms,[8] all with octahedral clusters, and the mixed-endohedral $\{(C_2)_2OLu_9\}I_8$[9] with edge-sharing tetrahedral and octahedral clusters.

Endohedral transition metal atoms are not known for lutetium clusters so far. One major problem appears to be the high stability of lutetium oxide–halides that are frequently, if not ubiquitously, observed; we have determined the crystal structures of LuOBr and LuOI (both PbFCl

[a] Department für Chemie, Institut für Anorganische Chemie, Universität zu Köln,
Greinstraße 6, 50939 Köln, Germany
Fax: +49-221-470-5083
E-mail: gerd.meyer@uni-koeln.de
[b] Fakultät für Chemie, Anorganische Chemie I – Festkörperchemie und Materialien, Ruhr-Universität Bochum, 44780 Bochum, Germany
Fax: +49-234-32-14951
E-mail: anja.mudring@rub.de
[c] II. Physikalisches Institut, Universität zu Köln,
Zülpicher Straße 77, 50937 Köln, Germany
Fax: +49-221-470-6708
E-mail: valldor@ph2.uni-koeln.de

type).[10] Thus, great care has to be taken to exclude oxygen from these systems. In our ongoing efforts in this area, $\{Os_5Lu_{20}\}I_{24}$, a compound that is special for a number of reasons, has been obtained and is reported here.

Results and Discussion

A conproportionation reaction of lutetium triiodide and lutetium metal in the presence of metallic osmium in a sealed tantalum container at 850–1200 °C yielded (very) thin, moisture-sensitive black needles of $\{Os_5Lu_{20}\}I_{24}$ in high yield and some LuOI. The preferred growth of the crystals as needles reflects the chain structure of the compound. It is the second in a series that may be represented by the general formula $\{Z_nR_{4n}\}X_{4n+4}$, the first being $\{Ir_3Sc_{12}\}Br_{16}$.[5] There is also the related composition $\{Z_nR_{4n}\}X_{4n}$. Halides belonging to both formula types have the Z atom in an eight-coordinate environment of R, the corresponding polyhedra being square antiprisms and, in some cases, cubes.

Square antiprisms alone are found in the $\{Z_nR_{4n}\}X_{4n}$ type, for which the examples $\{SiTa_4\}Te_4$,[11] $\{OsR_4\}Br_4$ (R = Y, Er),[12] $\{OsSc_4\}Cl_4$, and $\{ReGd_4\}Br_4$ have been observed so far,[5] with 16 or 15 electrons for intra-cluster bonding scaled for one endohedral atom Z. In all structures, square antiprisms $\{ZR_8\}$ share two common opposite faces, $\{ZR_{8/2}\}$, to form infinite chains that are surrounded by telluride or halide and stacked in a tetragonal close-packed fashion, with more or less connections between the chains such that the needle-like growth is anticipated. The Z atoms form slightly angled equidistant chains with d(Os–Os) = 307.4 pm in $\{OsSc_4\}Cl_4$,[5] for example.

For the $\{Z_nR_{4n}\}X_{4n+4}$ "series", the following are known examples:

For n = 3, $\{Ir_3Sc_{12}\}Br_{16}$ and its derivative $\{Os_3Sc_{12}\}Br_{16}Sc$,[5] as well as the tellurides $\{Z_3Sc_{12}\}Te_8Sc_{2-x}$ (with Z = Ru, x = 0.79 and Z = Os, x = 0.18),[13] have been obtained. They all contain chains of square-face-sharing square antiprisms and cubes in a ratio of 2:1. As a consequence, the Z chains are no longer equidistant. The Z–Z distances between atoms in the square antiprisms are shorter than between antiprism and cube, for example 283.3 versus 302.7 pm in $\{Ir_3Sc_{12}\}Br_{16}$.[5] If the short distance is associated with an Ir–Ir 2c–2e bond, the total number of cluster-based electrons is reduced from 47 to 45, which results in 15 electrons when scaled to one endohedral atom.

For n = 4 ($\{Z_4R_{16}\}X_{20}$), an oligomeric structure is obviously competing with the chain alternative. $\{Ru_4Y_{16}\}Br_{20}$[14] and $\{Fe_4Sc_{16}\}Cl_{20}$[15] may serve as examples. In these halide-containing cluster complexes, R octahedra share common edges and the voids are filled with a Z atom, which is obviously small enough to have a coordination number of six. Thus, these examples do not really rule out that there might be a chain alternative.

For n = 5 ($\{Z_nR_{4n}\}X_{4n+4}$), we have found the first example, namely, $\{Os_5Lu_{20}\}I_{24}$. It crystallizes in the triclinic space group $P\bar{1}$ with lattice constants of a = 1173.3(2) pm, b = 1248.4(2) pm, c = 1411.9(2) pm, α = 99.15(1)°, β = 107.66(1)°, γ = 108.84(1)°. The cluster repeat unit along the chains contains four square antiprisms and one cube, all sharing common faces (Figure 1).

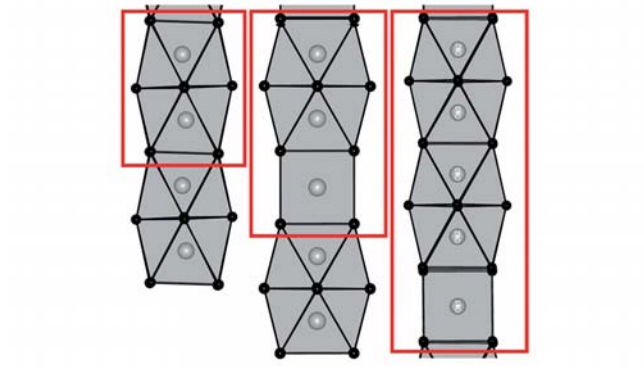

Figure 1. A comparison of the chains $\{Z_nR_{4n}\}$ (with n = 1, 3, 5) as observed (from left to right) in $\{OsSc_4\}Cl_4$, $\{Ir_3Sc_{12}\}Br_{16}$, and $\{Os_5Lu_{20}\}I_{24}$. The repeat units are indicated by red rectangles. Black circles represent R atoms, grey circles endohedral Z atoms.

Within the cubes in $\{Os_5Lu_{20}\}I_{24}$, Lu–Lu distances range from 334.0(3) to 346.7(2) pm with an average of 338.7 pm. The cubes are tetragonally elongated along the cluster chains, which run parallel [111]. Angles of the square faces deviate slightly from the ideal 90° by approximately –0.8°/+0.7°, torsion angles of the shared faces between neighbouring chain links are about 0.3°. The cubic voids are occupied by osmium atoms (Os1). The average Os–Lu distance amounts to 293.3 pm. Adjacent to the cubes, two square antiprisms of lutetium atoms (Lu2, Lu3) surround Os2. In the square antiprisms formed by (crystallographically) Lu2 atoms, Lu–Lu distances range from 334.0(3) to 336.9(2) pm in the rectangular faces and from 353.2(2) to 354.9(2) pm within the triangular faces with a total average of 344.9 pm. Angles found within the triangular faces vary between 56.2 and 62.0°, whilst those in the rectangular faces are between 89.6 and 90.4°. In contrast to the cubic surrounding, Os–Lu distances are significantly smaller with an average of 281.9 pm. The Os2–Lu_8 square antiprism shares the other face with an Os3–Lu_8 square antiprism. Lu–Lu distances range from 335.3(2) to 337.5(3) pm in the rectangular faces and from 350.1(2) to 352.50(18) pm within the triangular faces with an average of 344.0 pm. In accord with the aforementioned square antiprism, angles within the triangular faces vary from the ideal 60° between –3.1 and +1.8°. The common rectangular face between the two square antiprisms is nearly ideal. The average Os3–Lu distance is 281.5 pm. As there is a center of symmetry between two Os3 atoms, an $\{Os_5Lu_{20}\}$ unit emerges (Figure 1).

The $\{Os_5Lu_{20}\}$ cluster chains are surrounded by iodide ligands, capping edges (μ_2) or faces (μ_3), as shown in Figure 2. Some of the iodide ligands are only edge capping, exclusively with the cubes, whereas others are face capping, especially with the triangular faces of the square antiprisms. There are also iodide ligands that coordinate to four lutetium sites (Figure 2). Lu–I distances cover a wide range be-

tween 301.5(3) and 388.6(3) pm, with an average of 323.7 pm. This average, however, compares rather well with the Lu–I distances of 331.4(1) pm as observed in LuOI,[10] which appears to be the only reference available from single-crystal X-ray data. The $\{Os_5Lu_{20}\}I_{24}$ chains are packed in the fashion of a hexagonal closest packing of rods (Figure 2) just as in $\{Ir_3Sc_{12}\}Br_{16}$ but in contrast to $\{OsSc_4\}Cl_4$ (tetragonal packing). There are no significant interactions between the chains, other than van der Waals contacts, as the shortest inter-chain Lu–I distance of 467.9(3) pm attests. This feature is also seen in $\{Ir_3Sc_{12}\}Br_{16}$[5] and in $\{SiTa_4\}Te_4$.[11]

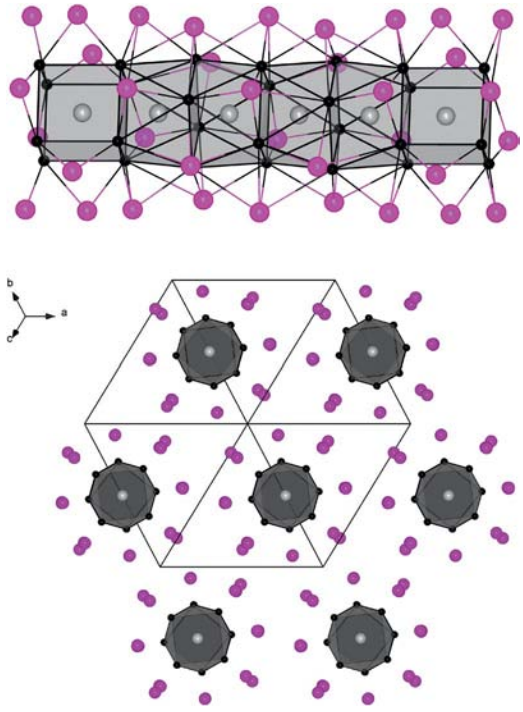

Figure 2. $\{Os_5Lu_{20}\}$ cluster chains surrounded by μ_2 and μ_3 bridging ligands in $\{Os_5Lu_{20}\}I_{24}$ (top) and their packing viewing down [111] (bottom).

An important feature of the crystal structure of $\{Os_5Lu_{20}\}I_{24}$ are the three different Os–Os distances that alternate along the chain of endohedral osmium atoms, with Os1 residing inside a cube, and Os2 and Os3 inside square antiprisms. The distances are 325.0(1) (Os1–Os2), 302.9(1) (Os2–Os3), and 298.8(1) pm (Os3–Os3). Angles along the osmium chain are 179.5 (Os2–Os3–Os3) and 180.0° (Os2–Os1–Os2). For one formula $\{Os_5Lu_{20}\}I_{24}$ unit, there are 76 electrons available for intra-cluster, mainly Os–Lu, bonding. If the situation were identical with that in $\{Ir_3Sc_{12}\}Br_{16}$, 75 electrons, or 15 scaled to one endohedral atom, would be the "magic" number for $\{Os_5Lu_{20}\}I_{24}$. This would leave only one electron for Os–Os bonding; the distances are indeed longer than the shortest Ir–Ir distance in $\{Ir_3Sc_{12}\}Br_{16}$ [283.28(9) pm].[5] Such a strictly local picture, however, is certainly too simple to interpret the bonding situation in a compound as complex as $\{Os_5Lu_{20}\}I_{24}$.

Thus, to obtain better insight, the electronic structure of $\{Os_5Lu_{20}\}I_{24}$ was calculated using the extended Hückel method. The density of states (DOS) interpreted by a projected density of states (PDOS) analysis shows that the Lu-4f levels are located well below the Fermi level. Contributions closer to the Fermi level are of Lu-5d and Os-5d character together with some minor contributions of Os-6s (at lower energies) and Os-6p levels as well as I-6p (Figure 3, left). This area can be divided into two sections. The area at lower energies (–14 to –8 eV) is mainly made up by I-6p together with Os-5d and Lu-5d states; the area close to the Fermi level contains mainly Lu-5d contributions with some minor contributions from Os-6p and I-6p states.

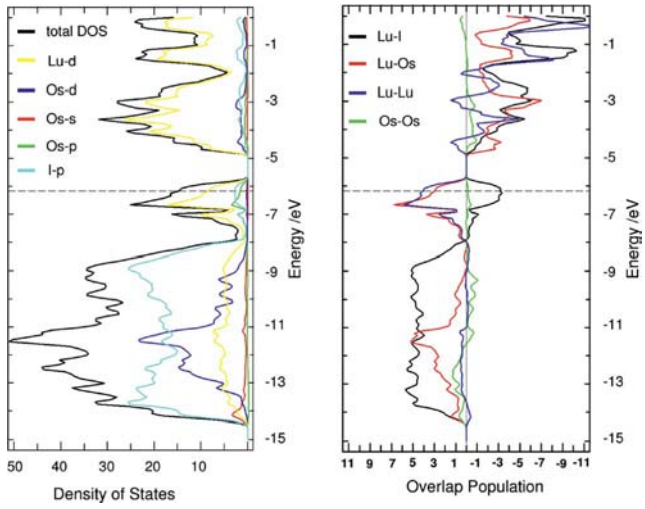

Figure 3. DOS with PDOS analysis for Lu-d (yellow), Os-d (blue), Os-s (red), Os-p (green), and I-p (cyan) contributions (left). COOP curve for Lu–I (black), Lu–Os (red), Lu–Lu (blue), and Os–Os (green) interactions (right).

The interpretation of bonding interactions by a crystal orbital overlap population (COOP) analysis shows that the major contributions come from bonding Lu–I and Lu–Os states (Figure 3, right). Above the pseudogap, around –8 eV, there are strongly bonding Lu–Lu as well as Lu–Os interactions together with Lu–I anti-bonding interactions close to the Fermi level. As already expected from the large interatomic distances, Os···Os interactions play a negligible role in the total bonding.

This bonding picture, that is, strong Z–R and R–X bonding with minor Z–Z and R–R contributions as well as R–X anti-bonding interactions close to the Fermi level, has been seen in many cases recently.[3f,4–6] New in the present case is the considerable population of Lu-5d states associated with Lu–Lu bonding interactions close to the Fermi level. Of the total number of 548 valence electrons of $\{Os_5Lu_{20}\}I_{24}$, 280 are located in Lu-4f orbitals. Roughly 45 electrons are in Lu-5d and Os-5d states, with almost 5 in the Os-6s state. These electrons, distributed evenly over five Os and twenty Lu atoms, would amount to electronic con-

figurations of $6s^15d^9$ for Os and $5d^{2.2}$ for Lu. This has to be taken into account when the magnetic susceptibility (Figure 4) is interpreted.

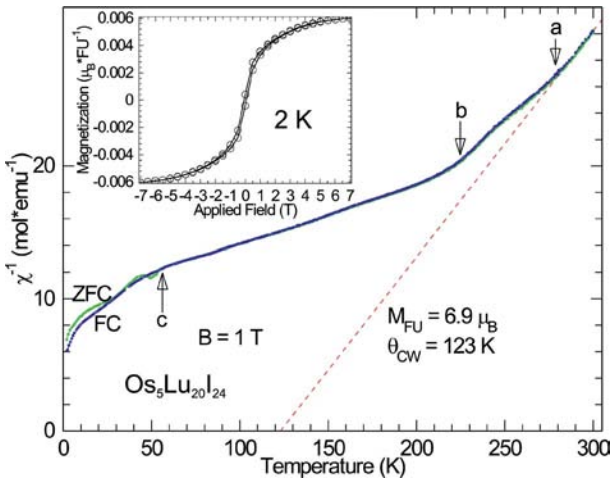

Figure 4. Reciprocal magnetic suscpetibility of $Os_5Lu_{20}I_{24}$ as a function of temperature. Field-cooled (FC, blue) and zero-field-cooled (ZFC, green) data are presented. The dashed line represents a Curie–Weiss fit from the high temperature range (275–300 K). Three anomalies in the curves are indicated with arrows and letters. The upper left inset displays the field dependent magnetization at 2 K in μ_B per formula unit (FU).

In principle, osmium and lutetium could be expected to possess half filled orbitals in $\{Os_5Lu_{20}\}I_{24}$, therefore evoking magnetism. The magnetism of 5d elements is often complex and the size of orbital contributions to the spin moment is difficult to predict. Above 280 K, the sample is assumed to be paramagnetic as the inverse susceptibility (χ^{-1}) is linearly proportional to the temperature (Figure 4). From a Curie–Weiss fit, a magnetic moment of about 7 μ_B per formula unit can be estimated. Depending on the degree of Os–Os, Os–Lu, and Lu–Lu bonding discussed above, a part of the possible magnetic moment could be cancelled out by singlet states. This makes it impossible to estimate spin or orbital moments without spectroscopic measurements. The positive Weiss constant (123 K), however, reveals a tendency towards ferromagnetic coupling between the Os/Lu spins. Ferromagnetic coupling is often found in combination with electronic conduction and the bonding situation in $\{Os_5Lu_{20}\}I_{24}$ is partly covalent. If $\{Os_5Lu_{20}\}I_{24}$ were to be metallic, even more magnetic moment would be lost due to electron delocalization and the compound would instead exhibit Pauli paramagnetic properties. Obvious paramagnetic behavior is observed meaning that parts of the electrons are localized in d- (or f-) orbitals. Moreover, the compound is black, which means that the band gap should to be smaller than the lowest photon energy in the visible light region (< 1.2 eV, $\lambda \approx 1000$ nm). These observations suggest that $\{Os_5Lu_{20}\}I_{24}$ is a semiconductor. The exact size of the band gap has to be investigated by means of temperature-dependent resistivity measurements.

Three anomalies in χ^{-1}, marked a–c in Figure 4, are observed close to 278, 223, and 57 K, respectively. Both high-temperature transitions indicate that more anti-ferromagnetic spin–spin couplings are formed. The spin ground state, below 57 K, contains clusters as evidenced by the observation of spin-state degeneracy (FC $\neq$ ZFC).

Several scenarios are possible to interpret the magnetic susceptibility vs. temperature, but, in combination with the quasi 1D magnetic sublattice in the crystal structure (Figure 2), the following events would describe the data well. At high temperatures, the 1D osmium/lutetium columns behave ferromagnetically but cannot order over a long range, probably because the spins are not Ising like. As the columns start to magnetically interact below 287 K, they prefer to align antiparallel. Due to the almost triangular arrangement of columns (Figure 2), the long-range anti-ferromagnetic spin order is prevented by geometric frustration. Hence, the spin system cannot order and the persisting spin fluctuations now contain a combination of ferro- and antiferromagnetic couplings. On passing the lowest transition c, the whole spin system freezes resulting in a cluster glass.[16]

The magnetization data (inset in Figure 4) can be described with a Brillouin function and reveal a small paramagnetic impurity, also explaining the tail seen below 10 K in the magnetic susceptibility. The amount of impurity can tentatively be estimated from the size of the saturation moment at 2 K. If the magnetization signal originates purely from an impurity it corresponds to 0.1% of the whole paramagnetic moment, as obtained from the Curie–Weiss fit. Hence, the impurity can be estimated to be present in about the same amount, which is far below detection limits of X-ray powder diffraction and the sample can be considered as pure. Not minding the impurity, the relatively low magnetization at 7 T confirms the domination of anti-ferromagnetism in the spin ground state.

Conclusion

A new polar intermetallic cluster chain of face-sharing square antiprisms and cubes (4:1 ratio) of lutetium atoms with endohedral osmium atoms, $\{Os_5Lu_{20}\}$, isolated by iodide ligands, has been observed for $\{Os_5Lu_{20}\}I_{24}$. This is a new member of the series $\{Z_nR_{4n}\}X_{4n+4}$. The $\{Os_5Lu_{20}\}$ chains are surrounded by edge- and face-capping iodide anions. There are only van der Waals contacts between the hexagonally close-packed $\{Os_5Lu_{20}\}I_{24}$ chains. The electronic structure is dominated by Os–Lu and Lu–I bonding interactions with lesser Lu–Lu and only negligible Os–Os interactions. Remarkable is the considerable population of Lu-5d states associated with Lu–Lu bonding interactions close to Fermi level. The magnetic behavior is complex exhibiting three temperature-dependent anomalies in the magnetic susceptibility. The spin ground state can be described as a cluster glass of ferromagnetically coupled spin columns. The ground state degeneracy is caused by antiferromagnetic coupling between the triangular arrangement of columns, that is, geometric frustration.

Experimental Section

Synthesis: Starting materials for the synthesis of $\{Os_5Lu_{20}\}I_{24}$ were osmium powder (Chempur, Karlsruhe, Germany, 99.9%) and filings of lutetium metal (Smart Elements, Vienna, Austria, 99.99%) which were used as purchased. Lutetium triiodide was synthesized from the elements by a procedure reported in the literature.[17] In a typical reaction, a mixture of these starting materials in a molar ratio of Os/Lu/LuI_3 = 2:4:5 (for example 20.5 mg of Os, 37.8 mg of Lu, and 150 mg of LuI_3) was placed, under dry-box conditions (MBraun, Garching, Germany; nitrogen, partial pressures of O_2 < 1 ppm and of H_2O < 0.5 ppm), into pre-cleaned tantalum containers that were sealed by He-arc welding and jacketed in silica ampoules.[18] The temperature program was as follows: Heat to 1200 °C, anneal for 3 d, cool at a rate of 2 °C/h to 850 °C, and, after 13 d, cool to ambient temperature at a rate of 7.5 °C/h. After the reaction was complete, the tantalum ampoule was opened in the dry box and inspected under a microscope. The vast majority of the sample consisted of small, (very) thin black, moisture-sensitive needles of what turned out to be $\{Os_5Lu_{20}\}I_{24}$. A very small amount of white by-products, presumably LuOI and unreacted LuI_3, were observed and could not be seen in the X-ray powder pattern.

Crystal Structure Determination: Needle-like crystals were selected and secured in sealed thin-walled glass capillaries. They were inspected by Laue photographs (Mo-K_α radiation, image plate) and the best specimen was transferred to a Stoe "Image Plate Diffraction System" (IPDS-II) and a complete data set was recorded. The data were corrected for Lorentz and polarization effects. A numerical absorption correction based on crystal-shape optimization was applied for all data. The programs used are Stoe's X-Area, including X-RED and X-Shape for data reduction and absorption correction, and SHELXS-97 and SHELXL-97 for structure solution and refinement.[19] The last cycles of refinement included atomic positions and anisotropic thermal parameters for all atoms. Details of the crystal structure investigations may be obtained from the Fachinformationszentrum Karlsruhe, 76344 Eggenstein-Leopoldshafen, Germany (Fax: +49-7247-808-666; E-mail: crysdata@fiz-karlsruhe.de), on quoting the depository number CSD-421639 for $\{Os_5Lu_{20}\}I_{24}$.

Crystal Data for $\{Os_5Lu_{20}\}I_{24}$: Triclinic, space group $P\bar{1}$ (No. 2); a = 1173.30(17) pm, b = 1248.41(17) pm, c = 1411.9(2) pm, α = 99.145(11)°, β = 107.663(11)°, γ = 108.844(11)°, V = 1787.7(4) × 10^6 pm^3; Z = 1; 1.58° < θ < 27.28°; Mo-K_α radiation (graphite monochromator, λ = 71.073 pm); T = 293(2) K; $F(000)$ = 3072; μ = 46.514 mm^{-1}; 14850 reflections measured, 7878 unique, 4023 observed. R_{int} = 0.0692, $R1/wR2$ = 0.0528/ = 0.1244 [$I_0 > 2\sigma(I_0)$] and 0.1032/0.1347 [all data]; Goodness-of-fit on F^2 = 0.922.

Magnetism: The magnetic susceptibility and magnetization data were obtained with a standard MPMS-XL from Quantum Design using fields up to 7 T in the temperature range 2–300 K. Due to the air sensitivity of the synthesized sample, the preparation for the magnetic measurement were completed in an Ar-filled glove box. As sample holder, a hard-gelatin capsule was used with an airtight lid.

Electronic Structure: Semi-empirical extended Hückel calculations (EH) were performed with the program package CAESAR[20] using double-ζ functions with the following parameters: Hij [eV], ζ_1, coefficient 1, ζ_2, coefficient 2. For Lu: 6s, –7.48, 1.95, 0.5602, 1.1, 0.5769; 6p, –3.09, 1.51, 1.0, 0.0, 0.0; 5d, –6.4, 2.8, 0.52, 1.15, 0.64; 4f, –18.129999, 12.0, 0.4543, 5.9, 0.6901. For Os: 6s, –9.54, 2.3, 0.5765, 1.251, 0.5533; 6p, –3.39, 1.77, 1.0, 0.0, 0.0; 5d, –11.24, 3.9, 0.6066, 1.85, 0.5486. For I: 5s, –22.41, 3.2, 0.6869, 1.95, 0.4869; 5p, –11.17, 2.65, 0.614, 1.45, 0.5258. A COOP analysis was used to interpret the chemical bonding.[21]

Acknowledgments

This work has been supported by the State of Nordrhein-Westfalen through the Universities of Cologne and Bochum. Especially noteworthy is the support by the Deutsche Forschungsgemeinschaft (DFG) to the Sonderforschungsbereich 608 ("Complex transition metal compounds with spin and charge degrees of freedom and disorder"). A. V. M. is grateful for the Dozentenstipendium awarded by the Fonds der Chemischen Industrie, Frankfurt/Main.

[1] a) J. D. Corbett, *Rev. Chim. Minerale* **1973**, *10*, 239–257; b) J. D. Corbett, *Acc. Chem. Res.* **1981**, *14*, 239–246; c) J. D. Corbett, *J. Chem. Soc., Dalton Trans.* **1996**, 575–587; d) J. D. Corbett, *Inorg. Chem.* **2000**, *39*, 5178–5191; e) J. D. Corbett, *J. Alloys Compd.* **2006**, *418*, 1–20; f) J. D. Corbett, *Inorg. Chem.* **2010**, *49*, 13–28.

[2] a) A. Simon, *Angew. Chem.* **1981**, *93*, 23–44; *Angew. Chem. Int. Ed. Engl.* **1981**, *20*, 1–22; b) A. Simon, *Angew. Chem.* **1988**, *100*, 163–188; *Angew. Chem. Int. Ed. Engl.* **1988**, *27*, 159–183; c) A. Simon, *Phil. Trans. R. Soc. A* **2010**, *368*, 1285–1299; d) A. Simon, Hj. Mattausch, G. J. Miller, W. Bauhofer, R. K. Kremer, in: *Handbook on the Physics and Chemistry Rare Earths* **1991**, *15*, pp. 191–285; e) A. Simon, Hj. Mattausch, M. Ryazanov, R. K. Kremer, *Z. Anorg. Allg. Chem.* **2006**, *632*, 919–929.

[3] a) G. Meyer, Th. Schleid, *Inorg. Chem.* **1987**, *26*, 217–218; b) G. Meyer, *Chem. Rev.* **1988**, *88*, 93–107; c) G. Meyer, H.-J. Meyer, *Chem. Mater.* **1992**, *4*, 1157–1168; d) G. Meyer, M. S. Wickleder, in: *Handbook on the Physics and Chemistry of Rare Earths* **2000**, *28*, pp. 53–129; e) G. Meyer, *Z. Anorg. Allg. Chem.* **2007**, *633*, 2537–2552; f) G. Meyer, *Z. Anorg. Allg. Chem.* **2008**, *634*, 2729–2736.

[4] N. Herzmann, A.-V. Mudring, G. Meyer, *Inorg. Chem.* **2008**, *47*, 7954–7956.

[5] S. Zimmermann, M. Brühmann, F. Casper, O. Heyer, T. Lorenz, C. Felser, A.-V. Mudring, G. Meyer, *Eur. J. Inorg. Chem.* **2010**, 2613–2619.

[6] S. Gupta, G. Meyer, J. D. Corbett, *Inorg. Chem.* **2010**, *49*, 9949–9957.

[7] H. Artelt, Th. Schleid, G. Meyer, *Z. Anorg. Allg. Chem.* **1992**, *618*, 18–25.

[8] Th. Schleid, G. Meyer, *Z. Anorg. Allg. Chem.* **1987**, *552*, 90–96.

[9] H. Mattfeld, K. Krämer, G. Meyer, *Z. Anorg. Allg. Chem.* **1993**, *619*, 1384–1388.

[10] a) S. Zimmermann, I. Pantenburg, G. Meyer, *Acta Crystallogr., Sect. E* **2007**, *63*, i156; b) S. Zimmermann, G. Meyer, *Acta Crystallogr., Sect. E* **2007**, *63*, i193.

[11] M. E. Badding, F. J. DiSalvo, *Inorg. Chem.* **1990**, *29*, 3952–3954.

[12] P. K. Dorhout, J. D. Corbett, *J. Am. Chem. Soc.* **1992**, *114*, 1697–1701.

[13] L. Chen, J. D. Corbett, *J. Am. Chem. Soc.* **2003**, *125*, 1170–1171.

[14] a) M. W. Payne, M. Ebihara, J. D. Corbett, *Angew. Chem.* **1991**, *103*, 842; *Angew. Chem. Int. Ed. Engl.* **1991**, *30*, 856; b) S. J. Steinwand, J. D. Corbett, *Inorg. Chem.* **1996**, *35*, 856.

[15] S. Zimmermann, Diplomarbeit, Universität zu Köln, **2006**; Dissertation, Universität zu Köln, **2008**.

[16] J. A. Mydosh, *Spin glasses: An experimental introduction*, Taylor & Francis, London, **1993**.

[17] a) J. D. Corbett, *Inorg. Nucl. Chem. Lett.* **1972**, *8*, 337–342; b) J. D. Corbett, *Inorg. Synth.* **1983**, *22*, 31–36; c) G. Meyer, in: *Synthesis of Lanthanide and Actinide Compounds* (Eds.: G.

Meyer, L. R. Morss), Kluwer Acad. Publ., Dordrecht, The Netherlands, **1991**, pp. 145–158.
[18] J. D. Corbett, *Inorg. Synth.* **1983**, *22*, 15–22.
[19] X-Shape 1.06, Crystal Optimisation for Numerical Absorption Correction (C), Stoe & Cie GmbH, Darmstadt, **1999**; X-Area 1.16, Stoe & Cie GmbH, Darmstadt, **2003**; X-RED 1.22, Stoe Data Reduction Program (C), Stoe & Cie GmbH, Darmstadt, **2001**; G. M. Sheldrick, *SHELXS-97 and SHELXL-97*, Programs for Crystal Structure Analysis, University of Göttingen, **1997**.
[20] J. Ren, W. Liang, M.-H. Whangbo, *CAESAR*, PrimeColor-Software Inc., Raleigh, NC, **1998**.
[21] S. Wijeyesekera, R. Hoffmann, *Organometallics* **1984**, *3*, 949.
Received: April 28, 2011
Published Online: August 2, 2011

